# Atomically precise rhodium nanoclusters: synthesis and characterization of the heterometallic $[Rh_{18}Sn_3Cl_2(CO)_{33}]^{4-}$ and $[Rh_7Sn_4Cl_{10}(CO)_{14}]^{5-}$ carbonyl compounds

Guido Bussoli [a], Cristiana Cesari [a], Cristina Femoni [a,*], Maria Carmela Iapalucci [a], Silvia Ruggieri [b], Cristina Tiozzo [a,1], Stefano Zacchini [a]

[a] *Department of Industrial Chemistry "Toso Montanari", University of Bologna, Viale del Risorgimento 4, 40136 Bologna, Italy*
[b] *Laboratory of Luminescent Materials, Department of Biotechnology, University of Verona, Strada Le Grazie 15, 37134 - Verona, Italy*

ARTICLE INFO

ABSTRACT

This paper presents a deepening on the investigation of the Rh-Sn system of heterometallic carbonyl clusters. More specifically, we herein report the synthesis and isolation of the new $[Rh_7Sn_4Cl_{10}(CO)_{14}]^{5-}$ (**1**) compound and the atomically precise $[Rh_{18}Sn_3Cl_2(CO)_{33}]^{4-}$ (**2**) nanocluster, where the la. Cluster **1** can be obtained by reacting the $[Rh_7(CO)_{16}]^{3-}$ homometallic cluster with hydrated Sn(II) chloride, in acetone; conversely, cluster **2** derives from the previously known $[Rh_{12}Sn(CO)_{23}Cl_2]^{4-}$ precursor after controlled addition of diluted sulphuric acid. Notably, only **2** has retained the recurrent Sn-centred icosahedral structural feature, while **1** shows a molecular structure based on two $Rh_4$ tetrahedra joint by one vertex and stabilized by $SnCl_2$ and $[SnCl_3]^-$ fragments. Both species have been characterized by infrared (IR) analysis in solution, single-crystal X-ray diffraction and Electrospray Ionization Mass Spectrometry (ESI-MS).

## Introduction

The preparation of atomically precise nanoclusters based on transition metal carbonyls has been widely explored in the last few years. [1] In the case of rhodium-based heterometallic species, the best strategy has turned out to be the redox condensation, [2] which combines two compounds containing the desired metals but with different reduction potentials, so to ensure the reaction driving force. When reacting together, they spontaneously produce a series of metal complexes and clusters, the latter usually with a higher nuclearity than that of the precursor. [3] This is mainly due to the high cohesion energy of Rh and the strength of Rh-CO bonds, [4] which enable the formation of large nanoclusters, stabilized by carbonyl ligands. [5].

Carbonyl clusters can be of interest in various fields, spanning from catalysis, [6] to biology [7] through nanoparticle preparation. [8] For instance, molecular intermetallic clusters represent good catalyst platforms due to their ordered structure and stoichiometric composition, which is known with atomic precision. Within the specificity of Rh-Sn systems, their combined activity in the form of bimetallic

nanoparticles has been exploited for electrocatalytic oxygen-reduction and ethanol-oxidation reactions. [9] Moreover, carbonyl ligand loss may occur in clusters (for instance promoted by temperature) making them potential candidates as CO-realising molecules (CORMs).

In consistence with our line of investigation on heterometallic Rh-based carbonyl nanoclusters, we herein report the synthesis and isolation of new Rh-Sn compounds, namely $[Rh_7Sn_4Cl_{10}(CO)_{14}]^{5-}$ (**1**) and $[Rh_{18}Sn_3Cl_2(CO)_{33}]^{4-}$ (**2**). The former has been obtained by reacting the $[Rh_7(CO)_{16}]^{3-}$ cluster precursor [10] with hydrated Sn(II) chloride, while the latter can be derived by controlled addition of diluted sulphuric acid to the $[Rh_{12}Sn(CO)_{23}Cl_2]^{4-}$ pre-formed heterometallic cluster. [11] The above-mentioned species have been characterized by infrared (IR) analysis in solution, single-crystal X-ray diffraction and Electrospray Ionization Mass Spectrometry (ESI-MS).

In the literature, the state-of-the-art shows tin derivatives coordinated to transition-metal carbonyl clusters (TMCC), therefore acting as ligands, for instance $M_3(CO)_6(\mu\text{-}SnPh_2)_3(SnPh_3)_3$ (M = Rh, Ir), [12] $Ru_6(CO)_{13}(C_6H_6)(SnPh_2)(C)$ [13] and $[Ir_6(CO)_{15}SnCl_3]^-$. [14] Much rarer are papers reporting the isolation of Rh-Sn carbonyl clusters where

tin is interstitially lodged inside the metal framework. To our knowledge, the only example is the icosahedral $[Rh_{12}Sn(CO)_{27}]^{4-}$, alongside with its derivatives obtainable by direct reaction with $SnCl_2$ under either CO ($[Rh_{12}Sn(RhCl)(CO)_{27}]^{4-}$) or $N_2$ ($[Rh_{12}Sn(CO)_{23}Cl_2]^{4-}$), [11] and by thermal CO cleavage ($[Rh_{12}Sn(CO)_{27-x}]^{4-}$ with $x = 1, 2$). [15] In all those cases, the tin atom is inserted in icosahedral cavities, which may be heavily or slightly distorted depending on the hetero- or homoleptic nature of the cluster, respectively. Notably, in the literature there are examples of naked Rh-Sn clusters where it is the Rh atom that is interstitially hosted in deltahedral frameworks described by Sn atoms, among which $[Rh@Sn_{12}]^{3-}$ and $[Rh_3@Sn_{24}]^{5-}$ [16].

## Materials and methods

**General Procedures**. All reactions were performed using standard Schlenk technique under either $N_2$ or CO. Solvents were dried and degassed before use; tetrahydrofuran (THF) was dehydrated with Na-benzophenone and distilled under $N_2$. [$NEt_4$]Cl and $SnCl_2$ were commercial products. $[Rh_7(CO)_{16}]^{3-}$ was prepared according to the literature. [10] IR spectra were recorded on a PerkinElmer Spectrum One interferometer in $CaF_2$ cells. Positive/negative-ion mass spectra were recorded in $CH_3CN$ solutions on a Waters Micromass ZQ 4000 using electrospray ionization. Experimental conditions: 2.56 kV ES-probe voltage, 10 V cone potential, 250 L/h flow of $N_2$ spray-gas, incoming-solution flow 20 μL $min^{-1}$.

**Molecular structure determination**. X-ray single-crystal diffraction experiments were performed on a Bruker Apex II diffractometer, equipped with a CCD (Charge Coupled Device) area detector, by using Kα-Mo radiation. Data were corrected for Lorentz polarization and absorption effects (empirical absorption correction SADABS [17]). Structures were solved by direct methods and refined by full-matrix least-squares based on all data using $F^2$. [18] Hydrogen atoms were fixed at calculated positions and refined by a riding model. All non-hydrogen atoms were refined with anisotropic displacement parameters, including disordered atoms, represented by one ammonium cation in **1** and some heavily disordered CO groups in **2**. In refining the crystal structure of **2**, the Platon function Squeeze was applied to account for acetonitrile solvent molecules that could not be modelled. All structure drawings were made with SCHAKAL99. [19] CCDC 2172029–2172030 contain the supplementary crystallographic data.

## Experimental

Synthesis of [$NEt_4$]$_5$[$Rh_7Sn_4Cl_{10}(CO)_{14}$]·2$CH_3CN$ ([$NEt_4$]$_5$**1**·2$CH_3$CN)

A solution of $SnCl_2$·2$H_2O$ (0.10 g, 0.53 mmol) in acetone (5 mL) was added to [$NEt_4$]$_3$[$Rh_7(CO)_{16}$] (0.63 g, 0.40 mmol) dissolved in 20 mL of the same solvent, under $N_2$. The resulting brown mother liquor was filtered. The mother solution contained [$NEt_4$]$_4$[$Rh_{12}Sn(CO)_{27}$]. The solid was dried under vacuum, washed with water (3 × 10 mL), ethanol (2 × 10 mL) and THF (2 × 10 mL) to eliminate [$NEt_4$][$Rh(CO)_2Cl_2$], then methanol (10 mL) for further purification. Finally, the residue was extracted with acetonitrile (20 mL). Precipitation by diffusion of hexane (1 mL) and di-isopropyl ether (20 mL) gave small red–purple crystals of [$NEt_4$]$_5$**1**·2$CH_3CN$ (yield around 15% based on Rh). The salt is soluble in acetonitrile, DMF and DMSO. $\nu$CO IR (acetonitrile): 1979s, 1971sh, 1838m $cm^{-1}$. Most relevant ESI-MS peaks: 1750, 971, 795 and 699 *m/z*.

Synthesis of [$NEt_4$]$_4$[$Rh_{18}Sn_3Cl_2(CO)_{33}$] ([$NEt_4$]$_4$**2**)

An acetonitrile solution of [$Rh_{12}Sn(CO)_{23}Cl_2$]$^{4-}$ was put under CO and controlled addition of diluted sulphuric acid was carried out, until the disappearance of the IR signals of the starting material. At the end, the mother solution was dried under vacuum, washed with water (2 × 10 mL), ethanol (2 × 10 mL) and THF (2 × 10 mL) to eliminate [$NEt_4$][$Rh(CO)_2Cl_2$], then methanol (10 mL) for further purification. The subsequent extraction in acetone isolated the already known [$Rh_{12}Sn$ $(RhCl)(CO)_{27}$]$^{4-}$, while **2** was extracted in acetonitrile. Precipitation by

diffusion of hexane (1 mL) and di-isopropyl ether (20 mL) into the solution gave black crystals of [$NEt_4$]$_4$**2** (yield around 10% based on Rh). The salt is soluble in acetonitrile, DMF and DMSO. $\nu$CO IR (acetonitrile): 1989s, 1863m $cm^{-1}$.

## Results and discussion

The redox condensation reaction performed on $[Rh_7(CO)_{16}]^{3-}$ upon addition of post-transition metal halides has been the object of investigations over the last decade. [3] The results of such studies highlighted the possibility of synthetising heterometallic rhodium nanoclusters of various nuclearity, depending on the reaction conditions. All chemical systems object of this analysis gave rise to the isoelectronic and isostructural $[Rh_{12}E(CO)_{27}]^{n-}$ species (n = 3 with E = Sb, [20] Bi; [21] n = 4 with E = Ge, [22] Sn [11]), whose structural feature consists of icosahedral Rh frameworks centred by the E element. Beyond that, different heterometallic systems behave differently upon addition of further $EX_n$ halide (X = Cl, Br). We decided to further investigate the Rh-Sn system, both by varying some reaction conditions and by performing some reactivity tests on the existing species.

More specifically, we carried out the reaction between $[Rh_7(CO)_{16}]^{3-}$ and hydrated $SnCl_2$ until a stoichiometric ratio of around 1:1.3, respectively, but in acetone as opposed to acetonitrile. While in acetonitrile, where both the reactants and all products are well soluble, the reaction with this stoichiometric ratio mainly leads to the formation of $[Rh_{12}Sn(CO)_{23}Cl_2]^{4-}$, in acetone a solid species precipitates and separates out from the mother solution, which contains $[Rh_{12}Sn(CO)_{27}]^{4-}$. After filtration and washing of the solid, extraction with acetonitrile and layering hexane onto the cherry-red solution, the new $[Rh_7Sn_4Cl_{10}(CO)_{14}]^{5-}$ cluster was obtained in crystalline form, albeit in poor yield.

The molecular structure of **1**, illustrated in Fig. 1, was determined through single-crystal X-ray diffraction. It consists of two $Rh_4$ tetrahedra sharing one vertex, each capped by a stannyl [$SnCl_3$]$^-$ fragment, acting as alkyl-like ligands, and joint by two carbene-like stannylene $SnCl_2$ units. The cluster is further stabilized by fourteen carbonyl ligands, of
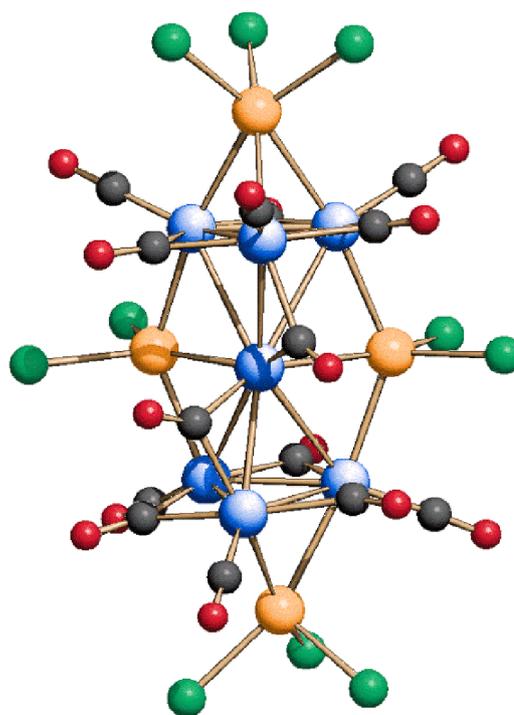


**Fig. 1.** Molecular structure of **1**. Rh atoms are depicted in blue, Sn atoms in orange, Cl atoms in green, C atoms in grey, O atoms in red.

which six terminally coordinated to every Rh atom, six edge-bridging the triangular Rh$_3$ edges, and the remaining two ligands bridging the Rh-Rh edges not connected by the SnCl$_2$ units.

Strictly speaking, the formation of the [Rh$_7$Sn$_4$Cl$_{10}$(CO)$_{14}$]$^{5-}$ species is not the result of a redox condensation, having both metals retained their oxidation states. In fact, considering the initial Sn(II) unaltered, the two SnCl$_2$ are neutral ligands, while the two [SnCl$_3$]$^-$ units bear a negative charge each. The former groups are two-electron donor ligands, whereas the latter units donate one electron each to the unsaturated [Rh$_7$(CO)$_{14}$]$^{3-}$ cluster, which in turn is four-electron short with respect to the [Rh$_7$(CO)$_{16}$]$^{3-}$ precursor. The final result is a penta-anionic species with 102 Cluster Valence Electrons (CVEs), given by the 9 Rh atoms, the anionic charge, the two-electron donor carbonyls and the Sn-bearing ligands. This number is in compliance with the Wade-Mingos electron-counting rules which, for a species composed of two metal tetrahedra joint by one vertex, predict a total $60 \times 2 - 18 = 102$ CVEs. [23].

The Rh-Sn and Rh-Rh bond distances are reported in Table 3S. While the latter are in line with those of other heterometallic compounds, the former are significantly, and expectedly, shorter if compared with those involving interstitial Sn in Rh icosahedral clusters.

The formation of **1** was quite unexpected as it had never been observed before during the reaction of [Rh$_7$(CO)$_{16}$]$^{3-}$ with SnCl$_2$ under N$_2$. In fact, in acetonitrile the reaction had been pushed up to a stoichiometry of 1:1.7, respectively, at which point cluster degradation was observed. As for intermediate stoichiometries, an equimolar ratio allowed to obtain [Rh$_{12}$Sn(CO)$_{23}$Cl$_2$]$^{4-}$, while a 1:1.5 ratio is known to give rise to the [Rh$_{12}$Sn(RhCl)(CO)$_{27}$]$^{4-}$ derivative, albeit under CO. However, the isolation of **1** may seem to suggest that this cluster could be a highly reactive intermediate in the reaction between [Rh$_7$(CO)$_{16}$]$^{3-}$ and SnCl$_2$, and its subtraction from the reaction medium, due to its insolubility in acetone, prevents it from reacting further. At the moment, this is only a hypothesis which would need to be confirmed with additional experiments.

Cluster **1** was also characterized by IR spectroscopy and ESI-MS. The corresponding spectra are reported in the Supporting Information (SI) section.

As aforementioned, some reactivity tests were performed on the already existing compounds with the aim of exploring different synthetic paths to obtain heterometallic species. As reactivity tests had been previously reported for the high-yield [Rh$_{12}$Sn(CO)$_{27}$]$^{4-}$ cluster, others were performed on the [Rh$_{12}$Sn(CO)$_{23}$Cl$_2$]$^{4-}$ derivative, which in turn can be originated by adding SnCl$_2$ to the parent [Rh$_{12}$Sn(CO)$_{27}$]$^{4-}$ under N$_2$ atmosphere, in fairly good yields. More specifically, we tried to oxidize the cluster through the addition of diluted sulphuric acid, with the purpose of generating new higher-nuclearity heterometallic species. In fact, among the different methods with which carbonyl clusters can be prepared, there is the formation of unstable hydride cluster through addition of H$^+$ and their subsequent rearrangement to larger species, with evolution of H$_2$. [24] In our case, the controlled addition of sulphuric acid to [Rh$_{12}$Sn(CO)$_{23}$Cl$_2$]$^{4-}$ under CO atmosphere led to the formation of a mixture of more oxidized products, among which [Rh(CO)$_2$Cl$_2$]$^-$, mostly, [Rh$_{12}$Sn(RhCl)(CO)$_{27}$]$^{4-}$, and traces of an unknown compound. The latter was purified and extracted with acetonitrile, then hexane was layered on top of the solution to afford slow precipitation of black crystals that, after X-ray diffraction analysis, allowed the identification of **2**.

The molecular structure of **2** is depicted in Fig. 2 and it is based on a distorted Sn-centred icosahedron of rhodium atoms onto which two additional {Rh$_3$SnCl} fragments are coordinated, on opposite sides. Thus, the icosahedral core of the parent [Rh$_{12}$Sn(CO)$_{27}$]$^{4-}$ has been retained. The cluster is further stabilized by thirty-three carbonyl ligands, and notably only those coordinated to the Rh atoms of the two additional {Rh$_3$SnCl} fragments are terminally coordinated, while the remaining ones are edge bridged.

This time, the Rh-Rh and Rh-Sn distances are completely in line with those observed in its [Rh$_{12}$Sn(CO)$_{27}$]$^{4-}$ congener.
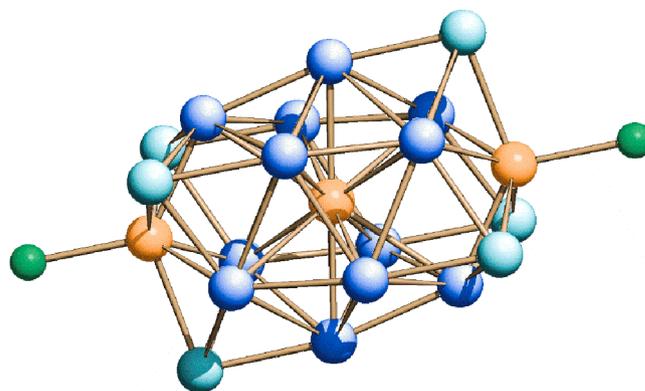


**Fig. 2.** Molecular structure of **2**. Rh atoms describing the icosahedral frame are depicted in blue, while the capping ones in pale blue, Sn atoms in orange, Cl atoms in green. The carbonyl groups have been omitted for sake of clarity.

Cluster **2** was also characterized by IR spectroscopy, $^1$H NMR and ESI-MS. Unfortunately, the latter was not diagnostic as the clusters heavily fragmented in the experimental conditions. As for the $^1$H NMR analysis, the results indicated the total absence of hydride signals.

This species represents an unexpected evolution in the Rh-Sn system, and it is its highest heterometallic nuclearity cluster, with dimensions of around $1.5 \times 1.0 \times 1.2$ nm. Moreover, [Rh$_{18}$Sn$_3$Cl$_2$(CO)$_{33}$]$^{4-}$ is structurally very similar to one of the Rh-Bi derivatives, namely [Rh$_{17}$Bi$_3$(CO)$_{33}$]$^{4-}$, which originates from the reaction between [Rh$_7$(CO)$_{16}$]$^{3-}$ with BiCl$_3$ in a 1:1.5 ratio. [21] More specifically, the Rh-Bi congener possesses, too, a Bi-centred icosahedral frame symmetrically capped by two additional Rh $-$ Bi $-$ Rh$_x$ fragments (x = 3/2). Within the highest-nuclearity Rh-E nanoclusters (E = Ge, Sn, Sb, Bi), these two compounds are undoubtedly the most similar ones in terms of metal framework. Their main difference lays on the lack of halides and one Rh atom in the Rh-Bi congener, while the number of carbonyl ligands and the negative charge are the same. The molecular structure of [Rh$_{17}$Bi$_3$(CO)$_{33}$]$^{4-}$ is illustrated in Fig. 3.

As for the electron counting, [Rh$_{18}$Sn$_3$Cl$_2$(CO)$_{33}$]$^{4-}$ reaches 242 CVEs given by all Rh atoms, the negative charge, the two three-electron donor [SnCl]$^+$ units and the carbonyl ligands. This value is in perfect agreement with the counting rules for an icosahedral cluster (170 CVEs)
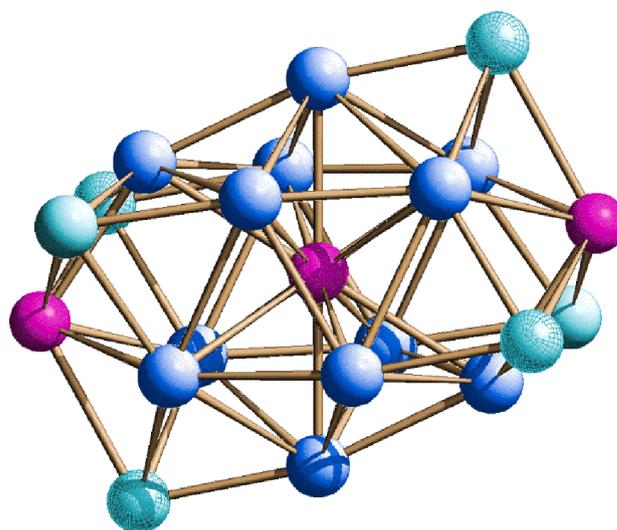


**Fig. 3.** Metal skeleton of [Rh$_{17}$Bi$_3$(CO)$_{33}$]$^{4-}$. Rh atoms describing the icosahedral frame are depicted in blue, while the capping ones in pale blue; Bi atoms are in magenta. The four hatched pale-blue Rh atoms possess a 75% occupancy factor as opposed to 100%, *de facto* giving rise to three atoms. The carbonyl groups have been omitted for sake of clarity.

capped by six Rh atoms (12 × 6 CVEs).

## Conclusions

In this paper we presented a further investigation of the Rh-Sn heterometallic cluster system, which resulted in the isolation and characterization of two new species, namely $[Rh_7Sn_4Cl_{10}(CO)_{14}]^{5-}$ (**1**) and $[Rh_{18}Sn_3Cl_2(CO)_{33}]^{4-}$ (**2**). The latter represents the highest nuclearity nanocluster within the Rh-Sn system, and it shows a Sn-centred icosahedral-based metal frame onto which additional heterometallic fragments coordinate. It also well fits into the category of atomically precise intermetalloid species, as it shows similarities to the structure of metals. [25]

The icosahedral structural feature shown by cluster **2** did not come as a surprise as it is very common in high-nuclearity TMCC. For instance, it has been observed in several Ni, [26] Pd, [27] and Pt derivatives, [28] not to mention the Au [29] and Ag-based [30] giant nanoclusters stabilized by thiolate ligands. One of the reasons, at least for heterometallic species, is that interstitial heteroatoms in icosahedral species have shown to impart extra stability to TMCC, even under reduction and oxidation reactions under electrochemical experiments. [31].

The obtained results demonstrate, once more, how the mechanism of metal-carbonyl cluster growth still continues to be a speculative aspect in this chemistry. In fact, while it may be possible to increase the cluster nuclearity by oxidizing a suitable precursor with acids, a slight difference in the reaction conditions may lead to the opposite result, that is in breaking down the cluster precursor into smaller compounds. [32] This may be the case for cluster **1**, but further experiments will be necessary in order to better understand its formation.

## Declaration of Competing Interest

The authors declare that they have no known competing financial interests or personal relationships that could have appeared to influence the work reported in this paper.

## Acknowledgment

## Appendix A. Supplementary data

Supplementary data to this article can be found online at https://doi.org/10.1016/j.rechem.2022.100435.

## References

[1] C. Femoni, C. Cesari, M. C. Iapalucci, S. Ruggieri, S. Zacchini. Group 9 and 10 Carbonyl Clusters. Editor(s): G. Parkin, K. Meyer, D. O'Hare. Reference Module in Chemistry, Molecular Sciences and Chemical Engineering, Elsevier, 2022, ISBN 9780124095472, (online). https://doi.org/10.1016/B978-0-12-820206-7.00151-7.

[2] (a) W.O. Hieber, E.H. Schubert, Absorptionsmessungen an Carbonylferrat-Lösungen im Sichtbaren und UV-Gebiet, Z. Anorg. Allg. Chem. 338 (1965) 32–36, https://doi.org/10.1002/zaac.19653380106;
(b) P. Chini, Large Metal Carbonyl Clusters (LMCC), J. Organomet. Chem. 200 (1980) 37–61, https://doi.org/10.1016/S0022-328X(00)88636-2.

[3] C. Femoni, M.C. Iapalucci, S. Ruggieri, S. Zacchini, From Mononuclear Complexes to Molecular Nanoparticles: The Buildup of Atomically Precise Heterometallic Rhodium Carbonyl Nanoclusters, Acc. Chem. Res. 51 (2018) 2748–2755, https://doi.org/10.1021/acs.accounts.8b00354.

[4] K. Wade, Metal-metal and metal-carbon bond energy terms for the rhodium carbonyl clusters $Rh_4(CO)_{12}$ and $Rh_6(CO)_{16}$, Inorg. Nucl. Chem. Letters 14 (1978) 71–74, https://doi.org/10.1016/0020-1650(78)80032-4.

[5] (a) D.S. Dolzhnikov, M.C. Iapalucci, G. Longoni, C. Tiozzo, S. Zacchini, C. Femoni, New High-Nuclearity Carbonyl and Carbonyl-Substituted Rhodium Clusters and Their Relationships with Polyicosahedral Carbonyl-Substituted Palladium and Gold-Thiolates, Inorg. Chem. 51 (2012) 11214–11216, https://doi.org/10.1021/ic3011508;
(b) C. Femoni, T. Funaioli, M.C. Iapalucci, S. Ruggieri, S. Zacchini, Rh-Sb

[6] (a) S. Zacchini, L.A. Berben, Metal carbonyl clusters of groups 8–10: synthesis and catalysis, Chem. Soc. Rev. 50 (2021) 9503–9539, https://doi.org/10.1039/D1CS00161B;
(b) A. Fasolini, S. Ruggieri, C. Femoni, F. Basile, Highly Active Catalysts Based on the $Rh_4(CO)_{12}$ Cluster Supported on Ce0.5Zr0.5 and Zr Oxides for Low-Temperature Methane Steam Reforming, Catalysts 9 (2019) 800, https://doi.org/10.3390/catal9100800;
(c) X. Du, R. Jin, Atomically Precise Metal Nanoclusters for Catalysis, ACS Nano 13 (2019) 7383–7387, https://doi.org/10.1021/acsnano.9b04533.

[7] A. Arrais, E. Gabano, M. Ravera, D. Osella, Transition metal carbonyl clusters in biology: A futile or niche research area? Inorg. Chimica Acta 470 (2018) 3–10, https://doi.org/10.1016/j.ica.2017.05.021.

[8] (a) L. Guczi, A. Beck, A. Horváth, D. Horváth, From Molecular Clusters to Metal Nanoparticles, Topics in Catalysis 19 (2002) 157–163, https://doi.org/10.1023/A:1015216205320;
(b) G. Schmid, D. Fenske, Metal clusters and nanoparticles, Phil. Trans. R. Soc. A 368 (2010) 1207–1210, https://doi.org/10.1098/rsta.2009.0281.

[9] (a) M. Ahn, I.Y. Cha, J. Cho, H.C. Ham, Y.-E. Sung, S.J. Yoo, Rhodium−Tin Binary Nanoparticle - A Strategy to Develop an Alternative Electrocatalyst for Oxygen Reduction, ACS Catal. 7 (2017) 5796–5801, https://doi.org/10.1021/acscatal.7b02402;
(b) M. Ahn, I.Y. Cha, J.K. Lee, S.J. Yoo, Y.-E. Sung, Heterogeneous rhodium–tin nanoparticles: highly active and durable electrocatalysts for the oxidation of ethanol, J. Mater. Chem. A 3 (2015) 17130–17134, https://doi.org/10.1039/C5TA02991K.

[10] S. Martinengo, P. Chini, Synthesis and characterization of the $[Rh_6(CO)_{15}]^{2-}$ and $[Rh_7(CO)_{16}]^{3-}$ anions, Gazz. Chim. It. 102 (1972) 344–354.

[11] C. Femoni, M.C. Iapalucci, G. Longoni, C. Tiozzo, S. Zacchini, B.T. Heaton, J. A. Iggo, Sn-centred icosahedral Rh carbonyl clusters: synthesis and structural characterization and $^{13}C-\{^{103}Rh\}$ HMQC NMR studies, Dalton Trans. 35 (2007) 3914–3923, https://doi.org/10.1039/B708469B.

[12] R.D. Adams, B. Captain, J.L. Smith, M.B. Hall, C.L. Beddie, C.E. Webster, Superloading of Tin Ligands into Rhodium and Iridium Carbonyl Cluster Complexes, Inorg. Chem. 43 (2004) 7576–7578, https://doi.org/10.1021/ic0489589.

[13] R.D. Adams, E. Trufan, Ruthenium–tin cluster complexes and their applications as bimetallic nanoscale heterogeneous hydrogenation catalysts, Phil. Trans. R. Soc. A 368 (2010) 1473–1493, https://doi.org/10.1098/rsta.2009.0277.

[14] L. Garlaschelli, F. Greco, G. Peli, M. Manassero, M. Sansoni, R. Della Pergola, A coordinatively flexible ligand for carbonyl clusters: bridging and terminal SnCl3 groups in the iridium clusters $[Ir_4(CO)_{11}(\mu\text{-}SnCl_3)]^-$, $[Ir_4(CO)_{10}(SnCl_3)(\mu\text{-}SnCl_3)]^{2-}$ and $[Ir_6(CO)_{15}(\mu_3\text{-}SnCl_3)]^-$, Dalton Trans. (2003) 4700–4703, https://doi.org/10.1039/B310790F.

[15] C. Femoni, M.C. Iapalucci, G. Longoni, C. Tiozzo, S. Zacchini, B.T. Heaton, J. A. Iggo, P. Zanello, S. Fedi, M.V. Garland, C. Li, The loss of CO from $[Rh_{12}(\mu_{12}\text{-}Sn)(CO)_{27}]^{4-}$: Synthesis, spectroscopic and structural characterization of the electron-deficient, icosahedral $[Rh_{12}(\mu_{12}\text{-}Sn)(CO)_{25}]^{4-}$ and $[Rh_{12}(\mu_{12}\text{-}Sn)(CO)_{26}]^{4-}$ tetra-anions, Dalton Trans. 2217–2223 (2009), https://doi.org/10.1039/B818944G.

[16] C. Liu, X. Jin, L.-J. Li, J. Xu, J.E. McGrady, Z.-M. Sun, Synthesis and structure of a family of rhodium polystannide clusters $[Rh@Sn_{10}]^{3-}$, $[Rh@Sn_{12}]^{3-}$, $[Rh_2@Sn_{17}]^{6-}$ and the first triply-fused stannide, $[Rh_3@Sn_{24}]^{5-}$, Chem. Sci. 10 (2019) 4394–4401, https://doi.org/10.1039/C8SC03948H.

[17] G.M. Sheldrick, SADABS, Program for empirical absorption correction, University of Göttingen, Germany, 1996.

[18] G.M. Sheldrick, SHELX97, Program for crystal structure determination, University of Göttingen, Germany, 1997.

[19] E. Keller, SCHAKAL99, University of Freiburg, Germany, 1999.

[20] (a) J.L. Vidal, J.M. Troup, $Rh_{12}Sb(CO)_{27}^{3-}$ An example of encapsulation of antimony by a transition metal carbonyl cluster, J. Organomet. Chem. 213 (1981) 351–363, https://doi.org/10.1016/S0022-328X(00)93970-6;
(b) C. Femoni, I. Ciabatti, M.C. Iapalucci, S. Ruggieri, S. Zacchini, Alternative synthetic route for the heterometallic CO-releasing $[Sb@Rh_{12}(CO)_{27}^{4-}$ icosahedral carbonyl cluster and synthesis of its new unsaturated $[Sb@Rh_{12}(CO)_{24}^{4-}$ and dimeric $[\{Sb@Rh_{12}Sb(CO)_{25}\}_2Rh(CO)_2PPh_3^{7-}$ derivatives, Progr. Nat. Sci.: Mat. Int. 26 (2016) 461–466, https://doi.org/10.1016/j.pnsc.2016.08.004.

[21] C. Femoni, G. Bussoli, I. Ciabatti, M. Ermini, M. Hayatifar, M.C. Iapalucci, S. Ruggieri, S. Zacchini, Interstitial Bismuth Atoms in Icosahedral Rhodium Cages: Syntheses, Characterizations, and Molecular Structures of the $[Bi@Rh_{12}(CO)_{27}]^{3-}$, $[(Bi@Rh_{12}(CO)_{26})_2Bi]^{5-}$, $[Bi@Rh_{14}(CO)_{27}Bi_2]^{3-}$, and $[Bi@Rh_{17}(CO)_{33}Bi_2]^{4-}$ Carbonyl Clusters, Inorg. Chem. 56 (2017) 6343–6351, https://doi.org/10.1021/acs.inorgchem.7b00409.

[22] A. Boccalini, P.J. Dyson, C. Femoni, M.C. Iapalucci, S. Ruggieri, S. Zacchini, Insertion of germanium atoms in high-nuclearity rhodium carbonyl compounds: synthesis, characterization and preliminary biological activity of the heterometallic $[Rh_{13}Ge(CO)_{25}]^{3-}$, $[Rh_{14}Ge_2(CO)_{30}]^{2-}$ and $[Rh_{12}Ge(CO)_{27}]^{4-}$ clusters, Dalton Trans. 47 (2018) 15737–15744, https://doi.org/10.1039/C8DT02466A.

[23] D.M.P. Mingos, Polyhedral skeletal electron pair approach, Acc. Chem. Res. 17 (1984) 311–319, https://doi.org/10.1021/ar00105a003.

[24] (a) S. Zacchini, Using Metal Carbonyl Clusters to Develop a Molecular Approach towards Metal Nanoparticles, Eur. J. Inorg. Chem. (2011) 4125–4145, https://doi.org/10.1002/ejic.201100462;
(b) V.G. Albano, D. Braga, P. Chini, D. Strumolo, S. Martinengo, New carbide

Nanoclusters: Synthesis, Structure, and Electrochemical Studies of the Atomically Precise $[Rh_{20}Sb_3(CO)_{36}^{3-}$ and $[Rh_{21}Sb_2(CO)_{38}^{5-}$ Carbonyl Compounds, Inorganic Chemistry 59 (2020) 4300–4310, https://doi.org/10.1021/acs.inorgchem.9b03135.

clusters in the cobalt sub-group. Part 10. Preparation and crystallographic characterization of dicarbido-octa-μ-carbonyl-hexadecacarbonyl-polyhedro-dodecarhodate(2–) as its bis(triphenyl-phosphine)iminium salt, [N (PPh$_3$)$_{22}$Rh$_{12}$C$_2$(CO)$_{24}$, J. Chem. Soc., Dalton Trans. (1983) 249–252, https://doi.org/10.1039/DT9830000249.

[25] (a) S. Zacchini, Using Metal Carbonyl Clusters to Develop a Molecular Approach towards Metal Nanoparticles, Eur. J. Inorg. Chem. (2011) 4125–4145, https://doi.org/10.1002/ejic.201100462;
(b) V.G. Albano, D. Braga, P. Chini, S. Strumolo, New carbide clusters in the cobalt sub-group. Part 10. Preparation and crystallographic characterization of dicarbido-octa-μ-carbonyl-hexadecacarbonyl-polyhedro-dodecarhodate(2–) as its bis(triphenyl-phosphine)iminium salt, [N(PPh$_3$)$_{22}$Rh$_{12}$C$_2$(CO)$_{24}$, J. Chem. Soc., Dalton Trans. (1983) 249–252, https://doi.org/10.1039/DT9830000249.

[26] C. Capacci, C. Cesari, C. Femoni, M.C. Iapalucci, F. Mancini, S. Ruggieri, S. Zacchini, Structural Diversity in Molecular Nickel Phosphide Carbonyl Nanoclusters, Inorg. Chem. 59 (2020) 16016–16026, https://doi.org/10.1021/acs.inorgchem.0c02572.

[27] N.T. Tran, D.R. Powell, L.F. Dahl, Nanosized Pd$_{145}$(CO)$_x$(PEt$_3$)$_{30}$ Containing a Capped Three-Shell 145-Atom Metal-Core Geometry of Pseudo Icosahedral Symmetry, Angew. Chem. Int. Ed. 39 (2000) 4121–4125, https://doi.org/10.1002/1521-3773(20001117)39:22<4121::AID-ANIE4121>3.0.CO;2-A.

[28] I. Ciabatti, C. Femoni, M.C. Iapalucci, G. Longoni, S. Zacchini, S. Zarra, Surface decorated platinum carbonyl clusters, Nanoscale 4 (2012) 4166–4177, https://doi.org/10.1039/C2NR30400G.

[29] N. Yan, N. Xia, L. Liao, M. Zhu, F. Jin, R. Jin, Z. Wu, Unraveling the long-pursued Au$_{144}$ structure by x-ray crystallography, Sci. Adv. 4 (2018) eaat7259, https://doi.org/10.1126/sciadv.aat7259.

[30] A. Desireddy, B.E. Conn, J. Guo, B. Yoon, R.N. Barnett, B.M. Monahan, K. Kirschbaum, W.P. Griffith, R.L. Whetten, U. Landman, T.P. Bigioni, Ultrastable Silver Nanoparticles, Nature 501 (2013) 399–402, https://doi.org/10.1038/nature12523.

[31] C. Cesari, C. Femoni, T. Funaioli, M.C. Iapalucci, I. Rivalta, S. Ruggieri, S. Zacchini, Heterometallic rhodium clusters as electron reservoirs: Chemical, electrochemical, and theoretical studies of the centered-icosahedral [Rh$_{12}$E(CO)$_{27}$]$^{n-}$ atomically precise carbonyl compounds, J. Chem. Phys. 155 (2021) 104301, https://doi.org/10.1063/5.0061764.

[32] (a) B. Weinert, S. Mitzinger, S. Dehnen, (Multi-)Metallic Cluster Growth, Chem. Eur. J. 24 (2021) 8470–8490, https://doi.org/10.1002/chem.201704904;
(b) S. Mitzinger, L. Broeckaert, W. Massa, F. Weigend, S. Dehnen, Understanding of multimetallic cluster growth, Nat. Commun. 7 (2016) 10480, https://doi.org/10.1038/ncomms10480.